Article

Beta and gamma-cytoplasmic actins display distinct distribution and functional diversity

DUGINA, Vera, *et al*.

Abstract

Using newly generated monoclonal antibodies, we have compared the distribution of beta- and gamma-cytoplasmic actin in fibroblastic and epithelial cells, in which they play crucial roles during various key cellular processes. Whereas beta-actin is preferentially localized in stress fibers, circular bundles and at cell-cell contacts, suggesting a role in cell attachment and contraction, gamma-actin displays a more versatile organization, according to cell activities. In moving cells, gamma-actin is mainly organized as a meshwork in cortical and lamellipodial structures, suggesting a role in cell motility; in stationary cells, gamma-actin is also recruited into stress fibers. beta-actin-depleted cells become highly spread, display broad protrusions and reduce their stress-fiber content; by contrast, gamma-actin-depleted cells acquire a contractile phenotype with thick actin bundles and shrinked lamellar and lamellipodial structures. Moreover, beta- and gamma-actin depleted fibroblasts exhibit distinct changes in motility compared with their controls, suggesting a specific role for each isoform in cell locomotion. Our [...]

Reference

DUGINA, Vera, *et al*. Beta and gamma-cytoplasmic actins display distinct distribution and functional diversity. *Journal of cell science*, 2009, vol. 122, no. Pt 16, p. 2980-2988

DOI : 10.1242/jcs.041970
PMID : 19638415

β- and γ-cytoplasmic actins display distinct distribution and functional diversity

Vera Dugina[1], Ingrid Zwaenepoel[2,*], Giulio Gabbiani[2], Sophie Clément[2] and Christine Chaponnier[2,‡]

[1]Belozersky Institute of Physico-Chemical Biology, Moscow State University, Moscow, Russia
[2]Department of Pathology and Immunology, Faculty of Medicine, University of Geneva, CMU, Geneva, Switzerland
*Present address: Centre National de la Recherche, Scientifique (CNRS), UMR 144, Institut Curie, Paris, France
‡Author for correspondence (christine.chaponnier@unige.ch)

Accepted 26 May 2009
Journal of Cell Science 122, 2980-2988 Published by The Company of Biologists 2009
doi:10.1242/jcs.041970

Summary

Using newly generated monoclonal antibodies, we have compared the distribution of β- and γ-cytoplasmic actin in fibroblastic and epithelial cells, in which they play crucial roles during various key cellular processes. Whereas β-actin is preferentially localized in stress fibers, circular bundles and at cell-cell contacts, suggesting a role in cell attachment and contraction, γ-actin displays a more versatile organization, according to cell activities. In moving cells, γ-actin is mainly organized as a meshwork in cortical and lamellipodial structures, suggesting a role in cell motility; in stationary cells, γ-actin is also recruited into stress fibers. β-actin-depleted cells become highly spread, display broad protrusions and reduce their stress-fiber content; by contrast, γ-actin-depleted cells acquire a contractile phenotype with thick actin bundles and shrinked lamellar and lamellipodial structures. Moreover, β- and γ-actin depleted fibroblasts exhibit distinct changes in motility compared with their controls, suggesting a specific role for each isoform in cell locomotion. Our results reveal new aspects of β- and γ-actin organization that support their functional diversity.

Supplementary material available online at
http://jcs.biologists.org/cgi/content/full/122/16/2980/DC1

Key words: Actin isoforms, Actin network, Cytoskeleton

Introduction

Actins are a family of highly conserved cytoskeletal proteins that play fundamental roles in nearly all aspects of eukaryotic cell biology. In vertebrates, six actin isoforms, i.e. two striated muscle [α-skeletal (α-SKA) and α-cardiac (α-CAA)], two smooth muscle (α- and γ-SMA) and two cytoplasmic (β- and γ-CYA) actins are encoded by distinct genes (Vandekerckhove and Weber, 1978). Muscle actins are tissue specific and organized in contractile units, whereas β- and γ-CYA are ubiquitous and essential for cell survival (Harborth et al., 2001). All actin isoforms exhibit highly conserved primary amino acid sequences with the main differences located at the extreme N-terminus. In particular, the two cytoplasmic actins (CYAs) differ only by four amino acids located at positions 1, 2, 3 and 9.

Contrary to what is known for muscle actins (Chaponnier and Gabbiani, 2004; Lambrechts et al., 2004), little is known about the possible specific roles of β- and γ-CYA, probably because of embryonic lethality when CYAs are absent or mutated (Shawlot et al., 1998). To avoid the early lethal phase, a conditional-knockout approach using the Cre-loxP system has been recently employed to specifically ablate the expression of γ-CYA in skeletal muscle (Sonnemann et al., 2006). This represses the isoform expression in the costamere and results in a progressive myopathy (Sonnemann et al., 2006). Distinct localizations of *β-(ACTB)* and *γ-CYA* (*ACTG1*) mRNAs in several cell types (Hill and Gunning, 1993; Watanabe et al., 1998;Bassell et al., 1998) have suggested different spatioregulation for the two isoforms.

A crucial step to explore the specific biological roles of the two CYAs is documenting their subcellular localization. A few studies using polyclonal antibodies (Abs) both in cultured cells (Otey et al., 1986; Schevzov et al., 2005) and in vivo (Hofer et al., 1997; Yao et al., 1995) have previously attempted to investigate whether CYAs are sorted into different intracellular compartments; these studies are, however, limited by the cross-reactivity of γ-CYA Abs with α- and γ-SMA (Otey et al., 1986; Schevzov et al., 2005). Although β-actin monoclonal antibodies (mAbs) have been produced for many years (Gimona et al., 1994), the unavailability of a specific γ-CYA Ab has precluded the precise comparative appreciation of the sorting of the two isoforms.

The ability of cells to divide, move, generate contractile force and maintain shape is based upon specialized actin-containing structures. Numerous actin-binding proteins (ABPs) exert tight control over actin-filament stability and function. Among the ABPs, some link actin filaments in tight bundles and stress fibers, or in branched networks, and others anchor filaments to membranes (Winder and Ayscough, 2005). Specific CYA sorting in these different cellular structures has not been reported.

Using two newly developed mAbs, we investigated the subcellular localization of β- and γ-CYAs in quiescent cells and in models of spreading, migration, division and contraction. Moreover, we used selective inhibitors of actin nucleation pathways to study which pathway controls the distinct organization of β- and γ-CYAs. Finally, we explored the effects of silencing each of these isoforms using specific siRNAs. Our results bring new data in support of the assumption that β- and γ-CYAs play different functional roles.

Results

Characterization of anti-CYA antibodies

Mice were injected with the N-terminal nonapeptides of β- and γ-CYA. The β- and γ-CYA mAbs were selected by ELISA screenings using the isoform synthetic peptides and their specificity was confirmed by western blots (Fig. 1).

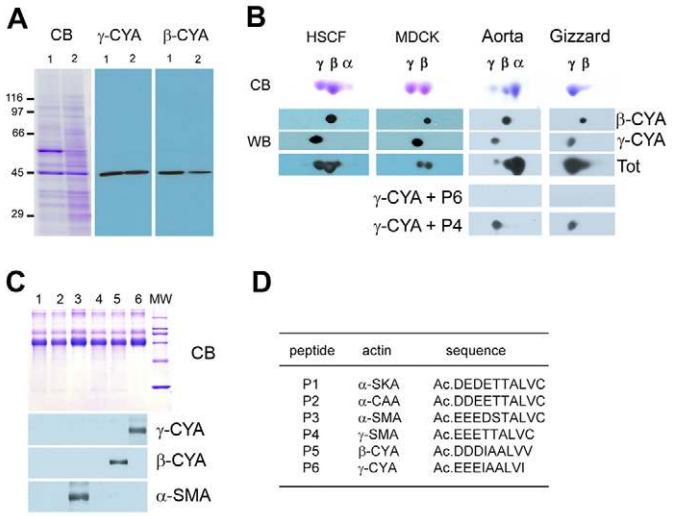

Fig. 1. Characterization of the β- and γ-CYA antibodies. (A) Total protein extracts from HSCFs (lanes 1) or MDCK cells (lanes 2) were subjected to SDS-PAGE, stained with Coomassie blue (CB) or blotted with β- or γ-CYA mAbs. Molecular mass in kDa is shown to the left. (B) Total protein extracts from HSCFs, MDCK cells, rat aorta or purified chicken gizzard actin were subjected to 2D PAGE, stained with Coomassie blue or blotted with β-CYA, γ-CYA and total actin (Tot) mAbs. Immunoblots of aorta extract or gizzard actin after 2D PAGE show that the mAb against γ-CYA only reacts with the more basic spot (γ). γ-CYA mAb was preincubated with the N-terminal peptide of γ-SMA or γ-CYA (P4 and P6 listed in D) before immunoblotting. Only the N-terminal peptide of γ-CYA (P6) blocks the immunoreactivity of the γ-CYA mAb. (C) Coomassie-blue-stained gel of the N-terminal peptides of the six mammalian actin isoforms listed in D, coupled to BSA. Immunoblots with β-CYA, γ-CYA and α-SMA mAbs show that each mAb reacts specifically with its corresponding peptide.

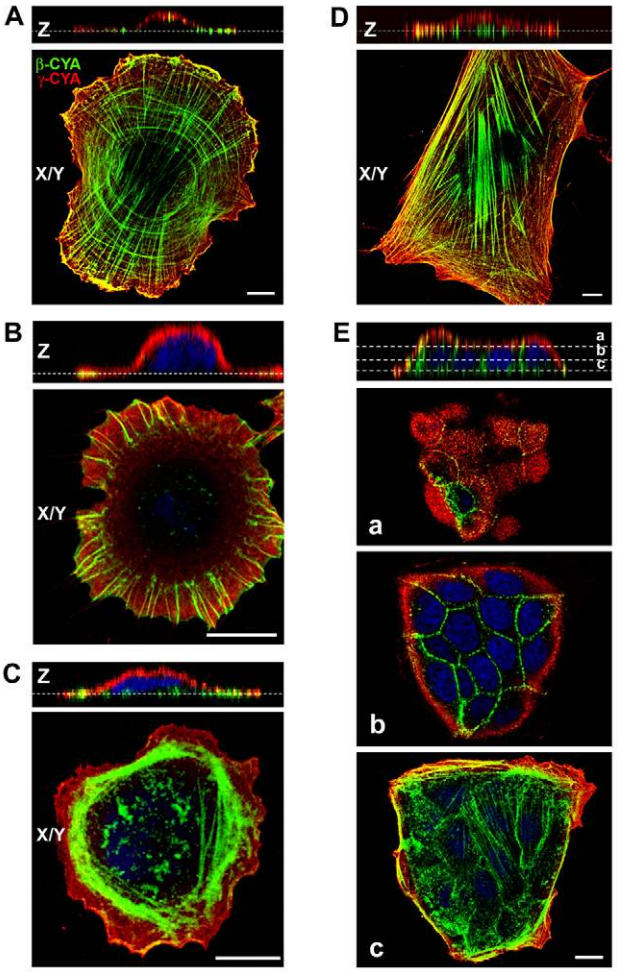

Fig. 2. β- and γ-actin are distributed in different arrays and cell compartments. (A-E) HSCFs (A,D), HaCaT cells (B) or MDCK cells (C,E) were plated for either 3 hours (A-C) or 3 days (D,E) and stained for β-actin (mAb 4C2) and γ-actin (mAb 2A3). Top images of each panel represent single *z*-sections. Dashed lines drawn in the top images indicate where the single *x/y* sections (bottom images) were generated. β-CYA is present in basal stress fibers (A,D,Ec), filopodia (B), cell-cell contacts (Eb) and circular bundles (A,C,Ec). γ-CYA is present in lamellar and dorsal cell regions. Yellow staining indicates zones of colocalization. Scale bars: 10 μm. See also separate channels in supplementary material Figs S1 and S2.

Immunoblots of human subcutaneous fibroblast (HSCF) and of Madin-Darby canine kidney (MDCK) epithelial cell extracts after western blot showed that the two mAbs recognized one single band at 42 kDa (Fig. 1A). Immunoblots of 2D PAGE using a pan-actin mAb revealed three spots (α, β and γ) in HSCFs and in rat aorta tissue extract, and two spots (β and γ) in MDCK cells and in purified chicken gizzard actin (Fig. 1B). Immunoblots of the same cell extracts incubated with the β- or γ-CYA mAb showed that each mAb recognized a single spot corresponding to the appropriate isoform (Fig. 1B). The specificity of the β-CYA mAb was clearly established owing to the unique isoelectric-point focusing of β-actin (Vandekerckhove and Weber, 1978). Because the N-terminal sequence AcEEE is identical in γ-CYA and in the two smooth muscle (SM) isoforms (see table in Fig. 1D), we have been attentive in controlling any possible cross-reaction of the γ-CYA mAb (Fig. 1B,C). ELISA screening, using plates coated with the peptides of α- and γ-SMA plus those of the two CYAs, was set up to eliminate Abs against common epitopes in different isoforms. Immunoblots of aorta extract after 2D PAGE showed that the mAb against γ-CYA did not cross-react with α-SMA (highly expressed in this case); moreover, peptide-blocking assay showed that the same mAb did not cross-react with γ-SMA (Fig. 1B). Only the γ-CYA peptide used originally to raise the mAb completely blocked the γ-CYA mAb reactivity when the γ-SMA peptide did not (Fig. 1B, aorta and gizzard).

The specificity of the mAbs was further characterized by checking their reactivity against the N-terminal peptides of the six mammalian actin isoforms coupled to bovine serum albumin (BSA) (Fig. 1D). Immunoblotting of these samples with the β-CYA and γ-CYA mAbs produced an exclusive reaction with their respective conjugated peptide (Fig. 1C), whereas anti-α-SMA mAb, used as a control, reacted specifically with the corresponding α-SMA peptide (Fig. 1C).

Subcellular localization of β- and γ-CYA in spreading and stationary fibroblastic and epithelial cells

We first monitored the organization of CYAs during cell spreading (Fig. 2A-C; supplementary material Fig. S1). In spreading HSCFs, γ-CYA was preferentially distributed into the cortical microfilament meshwork under the dorsal membrane and into the dendritic network at the lamellar periphery; β-CYA displayed a preferential localization in circular bundles and in radial stress fibers located at the ventral side of the cells (Fig. 2A). Spreading epithelial cells exhibited typical 'fried egg' morphology with circular protrusions composed of γ-CYA–network (Fig. 2B,C; supplementary material Fig. S1C). β-CYA

was organized in filopodia-like bundles (Fig. 2B) and in circular bundles (Fig. 2C; supplementary material Fig. S1B) at the basal side of the cell, whereas the γ-CYA staining was present at the apical part of the cell (Fig. 2C, *z*-section; supplementary material Fig. S1C).

In fibroblasts cultured for 3 days, β-CYA was mainly present in the stress fibers close to the substrate (Fig. 2D; supplementary material Fig. S2B), whereas those situated within the dorsal part of the cytoplasm contained γ-CYA (Fig. 2D, *z*-section; supplementary material Fig. S2C). In stationary fibroblasts showing reduced lamella and lamellipodia (e.g. after 7 days in culture or after TGFβ treatment), γ-CYA redistributed into stress fibers (data not shown). Considering reports describing different stress-fiber populations (Heath and Holifield, 1993; Pellegrin and Mellor, 2007; Small et al., 1998), our present observations suggest that β-CYA is preferentially distributed in arcs and ventral stress fibers (Fig. 2A,D; supplementary material Fig. S2B), and γ-CYA in dorsal stress fibers (supplementary material Fig. S2C). The same distribution of β-CYA in stress fibers was observed in fibroblasts transfected with β-actin–EGFP (supplementary material Fig. S3A).

After a few days in culture, epithelial cells organize in small islets by developing adhesions with their neighbors and generate cell polarity (Yeaman et al., 1999); protrusive activity only concerns regions free of contacts with other cells. In these conditions, β-CYA was preferentially distributed into: (1) stress fibers in the basal portion of the cytoplasm (Fig. 2Ec); (2) continuous cables at the cell periphery (Fig. 2Ec); and (3) thin short bundles at lateral cell-cell contacts (Fig. 2Eb and *z*-section). γ-CYA was mainly localized under the apical membrane (Fig. 2Ea and *z*-section) as well as in the protrusive regions around islets (Fig. 2Ec). Our observations indicate that β- and γ-CYA segregate, respectively, in basolateral- and apical-specific cell compartments. Similar results were observed in several fibroblastic, epithelial and endothelial cells (see all cell types studied in Materials and Methods) (not shown).

The permeabilization-fixation conditions used in this study are crucial for better accessibility of the N-terminus of actin isoforms (Schevzov et al., 2005). These conditions were particularly important in revealing the dendritic network with our newly developed γ-CYA mAb; other fixations, such as PFA–Triton-X-100 (TX), ethanol or methanol (MeOH) alone, allowed only a partial detection of both isoforms.

We compared the organization of β- and γ-CYA in normal human lung fibroblasts (WI38) and in their SV40-transformed counterparts (WI38-VA13) (supplementary material Fig. S4). In normal fibroblasts, β- and γ-CYA were organized in stress fibers and networks, respectively, as described above. By contrast, in transformed cells, stress fibers did not form and β-CYA was mainly distributed in ruffle and/or filopodia structures whereas the γ-CYA network became denser.

Organization of CYAs during cell migration

Directional migration was induced in fibroblastic and epithelial cells by scratching a confluent cell monolayer. We analyzed how actins spatially organize and participate in the formation of thin polarized membrane protrusions at the leading edge. In both cell types, protrusive lamellipodia were γ-CYA enriched (Fig. 3A; supplementary material Fig. S3B,C), compared with the cell body, which contained β-CYA organized in bundles close to the substrate (Fig. 3A; supplementary material Fig. S3B,C). Wound closure in epithelial cell sheets occurs by two distinct mechanisms: lamellipodia-dependent cell migration and coordinated purse-string contraction. Not all cells in the first row display this protrusive activity at the same time. A given cell may display protrusive activity, while another cell may be under tension with perimarginal actin bundles (Fenteany et al., 2000).

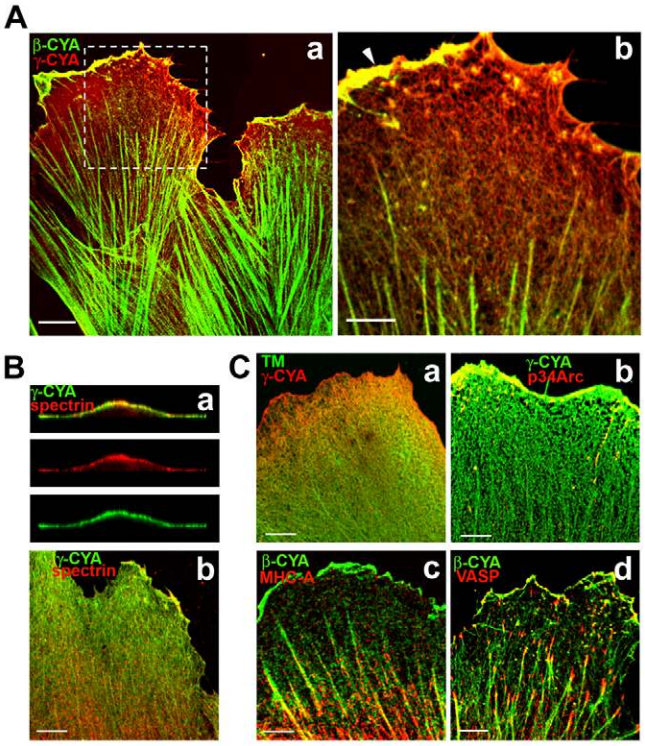

Fig. 3. β- and γ-actin display distinct distribution at the leading edge of cells moving into a wound. HSCFs were grown for 3 days in culture and experimental wounds were performed by scratching a cell monolayer. (A) At 3 hours after scratching, cells were stained for β-actin (mAb 4C2) and γ-actin (mAb 2A3). Image b represents higher magnification of the region delimited by the white frame in a. The yellow-colored ruffles indicate colocalization of both actin isoforms at the front of the leading edge in lamellipodia (arrowhead). Note a γ-CYA-network enrichment in protrusions of moving cells. (B,C) Co-distribution of CYAs with submembranous, lamellipodial and lamellar markers at the leading edge of moving HSCFs. The γ-CYA (mAb 4C2) network distributes with spectrin in the dorsal cortex (Ba), lamella and lamellipodia (Bb); with tropomyosin in lamella (Ca); and with p34Arc in lamellipodia (Cb). β-CYA (mAb 4C2) distributes with myosin IIA in contractile stress fibers (Cc). β-CYA (mAb AC-74) distributes with VASP in lamellipodia and in focal adhesions (Cd). Images represent *x/y* single sections. Scale bars: 10 μm (Aa), 5 μm (Ab,B,C). See also supplementary material Fig. S3.

During fibroblastic cell migration and spreading, dorsal and lamellipodial γ-CYA colocalized with the cortical marker spectrin (Fig. 3B) and the lamellar marker tropomyosin (TM, Fig. 3Ca). γ-CYA in lamellipodia was also colocalized with p34 Arc (Fig. 3Cb), a component of the Arp2/3 complex. β-CYA colocalized with myosin IIA in stress fibers (Fig. 3Cc), and with VASP in lamellipodia and focal adhesions (Fig. 3Cd).

Relationship between CYA segregation and actomyosin-based contractility

To study the relationship between actin organization and actomyosin contractility, we analyzed their distribution in dividing cells. In dividing human keratinocyte HaCaT cells (Fig. 4A), β-CYA was enriched in the equatorial region during anaphase (Fig. 4Aa) and at the contractile ring during telophase (Fig. 4Ab). γ-CYA was

located in the submembranous network (Fig. 4A). In spreading HSCFs, when compared with controls (Fig. 4B), treatment with blebbistatin, an inhibitor of non-muscle myosin II (Straight et al., 2003), induced the disappearance of β-CYA-containing stress fibers and arcs, with a denser network of γ-CYA (Fig. 4C).

Differential sensitivity of CYAs to small-GTPase inhibitors and actin-affecting drugs

The formation of stress fibers and lamellipodia is regulated by the small GTP-binding proteins RhoA and Rac1, respectively (Ridley and Hall, 1992; Ridley et al., 1992). Cell incubation with Y-27632, a selective inhibitor of Rho kinase (Uehata et al., 1997), resulted in the disorganization of β-CYA bundles, without disturbing the γ-CYA microfilament network (Fig. 4D). Incubation with the inhibitor of Rac1- GDP/GTP exchange activity, NSC23766 (Gao et al., 2004), hampered protrusive activity, as shown by loss of lamella and/or lamellipodia, disappearance of the γ-CYA dendritic network and enhanced formation of β- and γ-CYA stress fibers (Fig. 4E). To investigate the role of signaling pathways downstream of Rac1 in actin-isoform segregation, we used wiskostatin, a selective inhibitor of the neural Wiskott-Aldrich syndrome protein (N-WASP); this inhibitor prevents the activation of the Arp2/3 complex by maintaining N-WASP in an inactive, autoinhibited conformation (Peterson et al., 2004). Treatment with wiskostatin prevented the formation of γ-CYA-enriched lamellipodial protrusions (Fig. 4F). By contrast, wiskostatin-treated cells produced multiple β-CYA filopodia-like protrusions and ruffles (Fig. 4F) enriched by endogenous mDia1 and VASP (not shown). Interestingly, the mechanism of filopodium formation has recently been revised (Sarmiento et al., 2008). Although the N-WASP–Arp2/3-complex pathway was originally supposed to regulate filopodium formation, Sarmiento et al. found that the inhibition of either WAVE2 or Arp2/3 resulted in a decrease of lamellipodium and increase of filopodium formation. Moreover, inhibition of both WAVE2 and N-WASP increased active RhoA levels and resulted in the formation of mDia1-dependent filopodium formation (Sarmiento et al., 2008).

We also used cytochalasin D (CD), which binds to barbed ends of actin filaments with high affinity, and latrunculin A (LatA), which interacts with actin monomers and prevents their incorporation into filaments (Spector et al., 1989). Low doses of CD inhibited the formation of β-CYA stress fibers and caused β-CYA patches in spreading HSCFs (Fig. 4G). The localization of γ-CYA in lamellipodial protrusions (Fig. 4G) as well as the distribution of p34 Arc and Arp3 (not shown) were unaffected by CD. LatA

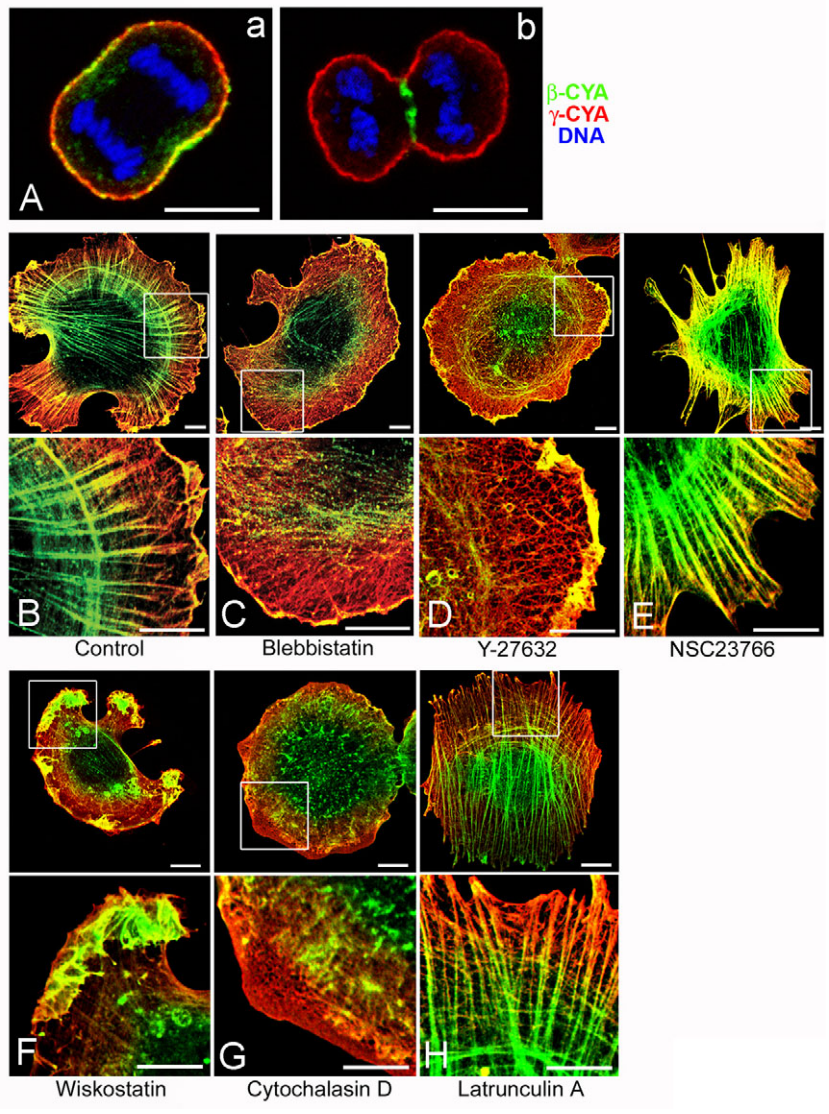

Fig. 4. β- and γ-actin are specifically located during mitosis and are under the control of different small GTPases and distinct polymerizing machinery. (A) β- and γ-CYA distribution during mitosis. Dividing HaCaT cells were stained for β-actin (mAb 4C2), γ-actin (mAb 2A3) and DNA (DRAQ5). β-CYA is enriched in the equatorial region of mitotic anaphase (a) and in the contractile ring in telophase (b), whereas γ-CYA only displays a submembranous staining. (B-H) HSCFs were allowed to spread for 7 hours and treated with myosin-II inhibitor (blebbistatin, C), RhoA-kinase inhibitor (Y-27632, D), Rac1-inhibitor (NSC23766, E), N-WASP-inhibitor (wiskostatin, F) or actin-destabilizing drugs [cytochalasin D (CD) in G; latrunculin (LatA) in H] and stained for β-actin (mAb 4C2) and γ-actin (mAb 2A3). Control without treatment is shown in B. Blebbistatin and Y-27632 treatment induces disorganization of β-CYA stress fibers and may slightly intensify the γ-CYA network. Both CYAs are still present in lamellipodia (yellow). NSC23766 treatment provokes dramatic thickening of β-CYA stress fibers, disappearance of the γ-CYA network from protrusions and recruitment of γ-CYA into stress fibers. Wiskostatin prevents γ-CYA-enriched lamellipodia formation and produces multiple β-CYA filopodia-like protrusions and ruffles. Capping barbed ends of actin filaments (CD) inhibits the formation of β-CYA stress fibers, whereas the localization of γ-CYA in lamellar and in lamellipodial protrusions is unaffected. Inhibition of actin-monomer incorporation into filaments (LatA) does not prevent the formation of β-CYA stress fibers, whereas γ-CYA lamellar and lamellipodial protrusions are poorly developed. Bottom panels show higher magnifications of the regions delimited by white frames on the top images. Single optical *x/y* sections are shown. Scale bars: 10 μm.

disrupted the γ-CYA network at the leading edge, but did not inhibit the formation of β-CYA stress fibers (Fig. 4H).

Effect of β- and γ-CYA silencing on cell morphology and motility

Subcutaneous fibroblasts

HSCFs were transfected with siRNA1 for *β-CYA* or *γ-CYA*, or with scramble siRNA as a negative control. Western blots for actins were performed 72 hours after siRNA transfection. The reduction of β-CYA by the specific siRNA was 31±4% (P<0.001), with no reduction of γ-CYA (Fig. 5A). The reduction of γ-CYA by the specific siRNA was 41±7% (P<0.001), with no reduction of β-CYA, but with an enhancement of α-SMA expression (Fig. 5A). It is noteworthy that, although the reduction of each isoform by siRNA was relatively modest, clear changes in cell morphology, polarity and motility were observed. This incomplete knockdown is probably due to the relatively long (2-3 days) half-life ($t_{1/2}$) of actin (Antecol et al., 1986). Our results suggest that a precise balance among isoform expression is mandatory for cell behavior and cannot be modified without resulting in profound cellular effects.

β- or γ-CYA-depleted cells displayed distinct morphological changes 72 hours after siRNA transfection: β-CYA-depleted cells exhibited broad protrusions at the leading edge, a clear reduction of stress fibers and β-CYA disappearance from lamellipodia, but persistence of the γ-CYA network (Fig. 5B; supplementary material Fig. S5A). γ-CYA-depleted cells did not generate lamellipodial protrusions and formed prominent bundles positive for β- and γ-CYA (Fig. 5B; supplementary material Fig. S5A) as well as for α-SMA (in 80% of depleted cells compared with 30% in control cells) (Fig. 5B, bottom panel, inset), thus assuming a 'contractile' phenotype. These results were similarly reproduced with other siRNA duplexes (siRNA2 and 3, see Materials and Methods) targeting the sequences of β-CYA and γ-CYA (supplementary material Fig. S5B), and using another fibroblastic cell line [human embryonic lung fibroblasts (HEL), not shown].

Morphometrical analysis showed that the average cell area was increased compared with controls after β-CYA silencing (from 2962±431 μm^2 to 5631±937 μm^2, P<0.01), but not after γ-CYA silencing. Circularity was increased after β-CYA silencing (from 0.360±0.005 to 0.545±0.020, P<0.001) and decreased after γ-CYA silencing (0.203±0.047, P<0.01).

Single-cell migration was studied 72 hours after *β-* or *γ-CYA* siRNA transfection. Cells were tracked at 5-minute intervals for 13 hours (Fig. 5C,D). Cells that divided or left the image field

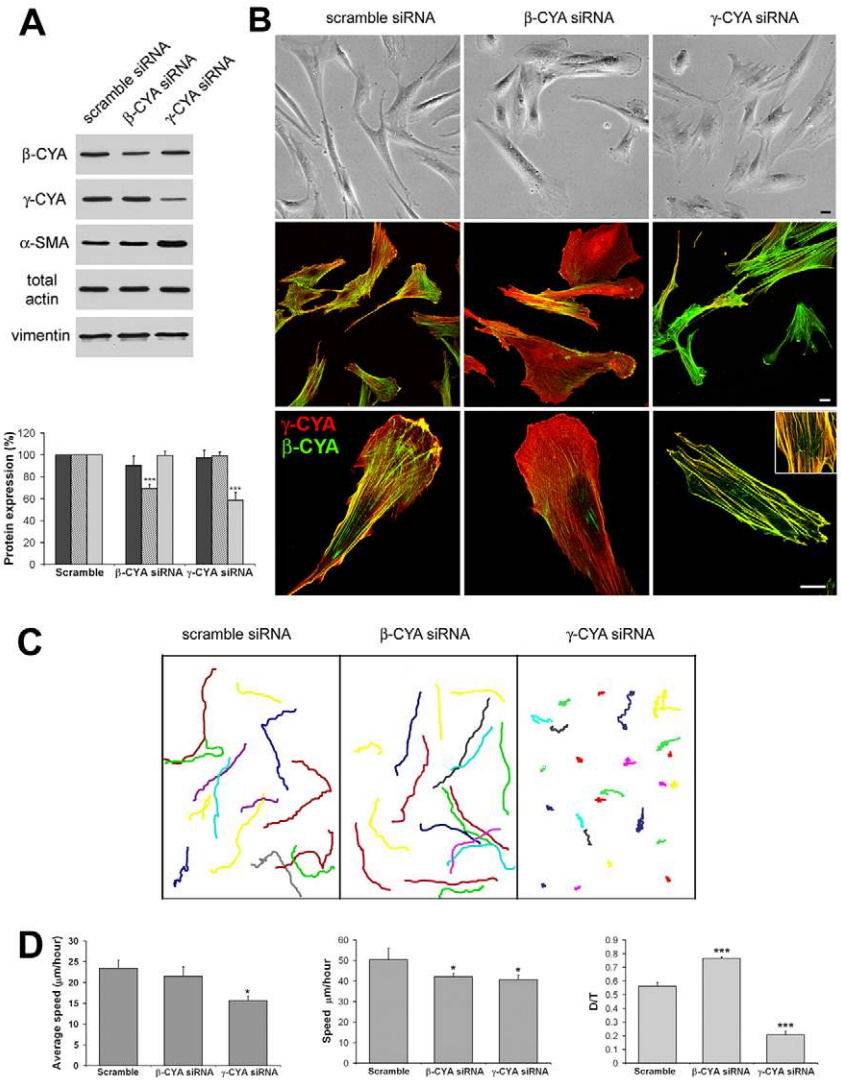

Fig. 5. A moderate depletion of β-CYA and γ-CYA is sufficient to affect cell morphology and motility. HSCFs were transfected with *β-CYA*, *γ-CYA* or scramble siRNAs. (A) Western blots were performed 72 hours after siRNA transfection using mAbs against β-CYA, γ-CYA, α-SMA, total actin and vimentin. Signals of total actin (black columns), β-CYA (hatched columns) and γ-CYA (grey columns) were quantified by densitometry and normalized using the vimentin signal as a reference protein. Data represent the mean ± s.e.m. of eight independent experiments. *β-CYA* and *γ-CYA* siRNA reduced the expression of their respective CYA. (B) Top images represent phase-contrast pictures of HSCFs 72 hours after siRNA transfection. β-CYA-depleted cells exhibit a leading edge with broad protrusions. γ-CYA-depleted cells display a contractile phenotype without lamellipodial protrusions. Middle and bottom panels represent HSCFs stained for β-actin (mAb 4C2) and γ-actin (mAb 2A3). The inset in the bottom panel shows staining for β-CYA and α-SMA. β-CYA depletion induces a significant reduction of β-CYA stress fibers. γ-CYA depletion reduces lamellar and lamellipodial protrusions, and induces prominent bundles of β-CYA enriched with α-SMA (inset). Scale bars: 20 μm. (C) Representative examples of migration tracks of cells 72 hours after *β-CYA* and *γ-CYA* siRNA transfection, recorded at 5-minute intervals for 13 hours. In these composite migration figures, randomly selected individual migration tracks were combined into a single figure. Differences in cell migration after depletion of each isoform were observed. Migration tracks are: long with a change of directionality at least once for the observation time in scramble control; shorter compared with control, but seem more persistent in their directionality after β-CYA depletion; short with multiple changes of the migration directionality after γ-CYA depletion. (D) Quantification of the speed and directionality of cell migration. See Materials and Methods for details and supplementary material Fig. S5.

during the experiment were not used for data analysis. We observed clear differences in cell migration after the depletion of each actin (Fig. 5C). Average speed, calculated during the total period of recording, was not different between control and β-CYA-depleted cells, but was significantly decreased in γ-CYA-depleted cells (~33% decrease) (Fig. 5D). Speed, calculated during periods of movement, was significantly reduced in both *β-CYA*- and *γ-CYA*-siRNA-treated cells (15-20% decrease) (Fig. 5D). Compared with controls, γ-CYA depletion reduced up to ~63% directional migration (Fig. 5D), measured as the ratio between the distance from start to end point (*D*) and the total track distance (*T*), whereas β-CYA depletion produced an enhancement (~35%) of this parameter. These results indicate that γ-CYA is responsible for the persistence of directional migration, whereas β-CYA could play a role in short-term motility.

The cell leading edge displayed different features according to the situation: protruding and retracting lamellipodia and numerous ruffles in scramble controls; continuous lamellipodial protrusions in β-CYA-depleted cells; and filopodia-like protrusions and cell-edge contraction in γ-CYA-depleted cells.

Kymograph analyses showed that β-CYA-depleted cells displayed smooth and persistent protrusions for long periods, whereas control cells exhibited periodic lamellipodial protrusions and retractions (supplementary material Fig. S5C). γ-CYA-depleted cells did not produce quantifiable protrusions (not shown).

Epithelial cells

HaCaT cells were transfected with siRNA for either *β-CYA* or *γ-CYA*, or with scramble siRNA. Western blots for actins showed that the reduction of β-CYA by the specific siRNA was 28±4% ($P<0.01$), whereas γ-CYA was slightly enhanced in the presence of *β-CYA* siRNA (9.5±5%, $P<0.05$). The reduction of γ-CYA by the specific siRNA was 35.5±6% ($P<0.01$), with no change of β-CYA (supplementary material Fig. S6A).

β-CYA-depleted cells exhibited a leading edge with broad protrusions; γ-CYA-depleted cells exhibited an elongated polygonal phenotype and no lamellipodial protrusions (supplementary material Fig. S6B). Immunofluorescence staining of β-CYA-depleted cells showed the reduction of β-CYA-positive stress fibers and of β-CYA bundles at the level of cell-cell contacts, but no alteration of the γ-CYA network (supplementary material Fig. S6B). The morphology of γ-CYA-depleted cells evolved towards a fibroblast-like contractile phenotype with the development of thick β-CYA positive stress-fibers (supplementary material Fig. S6Bc). Depletion of γ-CYA in these cells did not promote an expression of α-SMA. A few cells with blebs were also observed in γ-CYA-depleted HaCaT cells (supplementary material Fig. S6Bb, inset), validating the submembranous localization of γ-CYA and its role in cell-shape maintenance.

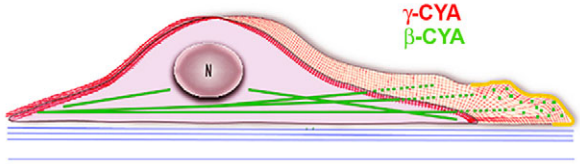

Fig. 6. Scheme summarizing the distribution of β- and γ-actin in a moving fibroblast. The two CYAs are organized in different arrays: γ-CYA as a branched meshwork in a cortical and lamellar localization; β-CYA as an unbranched filamentous array in stress fibers; β- and γ-CYA are colocalized in lamellipodia (yellow); blue lines represent substrate.

Furthermore, we observed that β-CYA silencing resulted in a high percentage of polynucleated cells (29±2%, $P<0.001$), compared with 2% in both scramble control and in γ-CYA-depleted cells (supplementary material Fig. S6C).

Discussion

The possibility that CYAs exert distinct biological functions has long remained an open question, despite evidence suggesting that muscle isoforms can play specific roles (Chaponnier and Gabbiani, 2004; Lambrechts et al., 2004). The present results, obtained by specific immunodetection of β- and γ-CYA in the same cell, demonstrate for the first time a clear-cut segregation of these isoforms in the cytoplasm of mesenchymal and epithelial cells during quiescence, as well as during locomotion and cytokinesis. Moreover, selective depletion of these isoforms indicates that each of them participates differently in the organization of cell morphology, polarity and motility.

Two actin filamentous arrays, i.e. bundles and branching networks, have been well characterized in non-muscle cells by electron microscopy (Abercrombie et al., 1971; Small, 1981; Svitkina et al., 1995) and immunolabeling techniques (Svitkina and Borisy, 1999). Bundles are present in stress fibers, filopodia, contractile rings and at cell-cell contacts, whereas branched filaments form the submembranous and the lamellar and/or lamellipodial meshwork (Chhabra and Higgs, 2007; Revenu et al., 2004; Winder and Ayscough, 2005). Our results show that each of these two filamentous arrays is characterized by the prevalence of β-CYA in bundles and of γ-CYA in branched filaments, as schematically illustrated in Fig. 6. This selective distribution is observed in all examined cell types, indicating that it represents a general cellular feature.

Our observations are partly in discordance with previous reports that show that β-CYA is mainly expressed at the leading edge (Gimona et al., 1994; Hoock et al., 1991), and that its mRNA is located in the lamella, proximal to the lamellipodia, where new translation takes place (Kislauskis et al., 1994). It is well accepted that accessibility of epitopes largely depends on fixation-permeabilization conditions; this might help to explain these discrepancies. After several tests, we decided to use PFA and MeOH (PFA/MeOH), which results in a regular and strong β-CYA stress-fiber staining, in addition to the previously described localization at the leading edge after PFA and TX (PFA/TX) fixation. Commercially available β-CYA mAbs after fixation with PFA/MeOH instead of PFA/TX stained stress fibers similarly to our antibody (Fig. 3Cd); thus, we suggest that the present results, showing for the first time an important incorporation of β-CYA into bundles, indicate that PFA/MeOH allows a more plausible detection of N-terminus actin isoform epitopes compared with the PFA/TX conditions. In this respect, it is noteworthy that β-CYA–GFP is also highly recruited in stress fibers (see supplementary material Fig. S3A). γ-CYA was also optimally stained when using PFA/MeOH.

In contrast to β-CYA (Gimona et al., 1994; Hoock et al., 1991), γ-CYA distribution was never described in epithelial and mesenchymal cells. Our new Abs allowed this investigation. Moreover, using recently developed γ-CYA Abs, it has been shown that, in skeletal muscle, γ-CYA localizes within the costamere (Hanft et al., 2006). This submembranous compartmentalization correlates with our results showing that dorsal cortical meshworks are mainly composed of γ-CYA.

Here, we provide several experimental approaches supporting the differential distribution of CYAs. (1) Our siRNA experiments

showed that β-CYA-depleted cells highly reduced their stress-fiber content, whereas γ-CYA-depleted cells did not generate lamellipodial protrusions. (2) The formation of stress fibers and lamellipodia is respectively regulated by the small GTP-binding proteins RhoA and Rac1 (Ridley and Hall, 1992; Ridley et al., 1992). We demonstrate that selective inhibitors of RhoA kinase and Rac1 specifically interfere with the distribution of β-CYA and γ-CYA. Interestingly, the site of β-CYA synthesis appeared to depend on Rho rather than on Rac or Cdc42 (Latham et al., 2001). (3) We also show that CYA filamentous arrays differentially respond to actin-depolymerizing drugs (CD and LatA). Such a differential sensitivity of cortical actin vs stress fibers to these drugs has previously been suggested (Lunn et al., 2000). The fact that CD, by capping the growing ends of actin filaments (Spector et al., 1989), leads to depolymerization of stress fibers is a strong argument in favor of β-CYA polymerization in stress fibers. By contrast, by sequestering monomeric actin (Spector et al., 1989), LatA seemed to inhibit selectively the formation of the γ-CYA network, suggesting that this pool of monomeric actin is necessary for the formation of branched filaments. (4) Finally, we found that a specific marker of lamellipodia (p34Arc, one member of the Arp2/3 family) co-distributed with γ-CYA, whereas β-CYA colocalized with VASP at the initiation site of polymerization.

An important cell feature involving actin organization is cell polarity, defined as asymmetry in cell shape, protein distribution and cell activity (Yeaman et al., 1999). In epithelial cells, plasma-membrane and cytoskeletal proteins are organized into apical and basolateral domains that are functionally and structurally distinct (Nelson, 2003; Yeaman et al., 1999). Our results demonstrate that β-CYA and γ-CYA are segregated in basolateral and in apical domains, respectively. siRNA experiments suggest a role of β- and γ-CYA for correct polarity formation: β-CYA-depleted cells lost organized cell-cell contacts; γ-CYA-depleted cells underwent epithelio-mesenchymal transition illustrated by the development of stress fibers.

In cultured fibroblasts, polarity is characterized by lamellipodial extension in the direction of migration at the front of the cell and by a narrow, retracting tail at the rear of the cell (Abercrombie et al., 1970). Scratch assays have demonstrated the gradual evolution from a contractile phenotype, with predominance of β-CYA-containing stress fibers in quiescent cells, to a motile phenotype with γ-CYA enrichment in lamellipodial protrusions. Interestingly, whereas β-CYA and γ-CYA are colocalized in lamellipodia, both isoforms coexist in the lamella and are distributed in their respective filamentous organization. Because *β-CYA* mRNA is abundantly located at the cell leading edge (Condeelis and Singer, 2005), we cannot exclude that, at least in part, β-CYA staining observed at the front of the leading edge represents newly synthesized β-CYA.

Our results in actin-depleted cells argue in favor of a crucial role for γ-CYA in the control of directional motility. In addition to cell polarization, other processes are involved in fibroblast migration: leading-edge extension, formation of cell-substrate attachments, traction of the cell body and release of attachments at the rear (Lauffenburger and Horwitz, 1996; Ridley et al., 2003). In this context, it is worth noting that protrusive activity was impaired in γ-CYA-depleted cells. β-CYA also plays a role in cell migration, because cell speed recorded during movement periods was significantly decreased in β-CYA-depleted cells.

Additional support for a role of CYAs in cell migration comes from our observations showing that transformed cells lose β-CYA-containing stress fibers and exhibit an increased γ-CYA-containing network. A major feature of cell transformation consists of reorganization of the actomyosin cytoskeleton, leading to increased cell motility and invasion. Numerous studies have shown the disappearance of stress fibers in transformed cells (Pawlak and Helfman, 2001; Pollack et al., 1975; Rubin et al., 1978; Verderame et al., 1980). Our results indicate that a specific change in actin isoform occurs in oncogenic transformation.

The sorting of β-CYA in myosin-dependent contractile bundles (stress fibers, circular bundles, contractile ring) suggests a role for this isoform in cell contraction. Blebbistatin, a specific inhibitor of myosin-II ATPase activity, lowers the affinity of myosin for actin, preventing actomyosin interaction (Kovacs et al., 2004). Specific suppression of contractility by blebbistatin induced the disappearance of β-CYA-containing stress fibers, but did not disturb the γ-CYA network. Myosin-IIA-depleted cells, as well as blebbistatin-treated cells, exhibited a phenotype with motile morphology, a decreased amount of stress fibers and a highly protrusive leading edge (Even-Ram et al., 2007; Sandquist et al., 2006). Blebbistatin abolishes cell tension, disassembles actin stress fibers and inhibits the association of myosin II with actin filaments (Goeckeler et al., 2008). We show that myosin inhibition by ROCK inhibitors or by blebbistatin strongly interferes with β-CYA stress-fiber formation. It is conceivable, albeit not-yet proven, that β-CYA and myosin IIA interact, as suggested by their colocalization.

Another argument in favor of a role of β-CYA in cell contraction is represented by its localization in the contractile ring during cytokinesis, whereas γ-CYA is distributed in the submembranous domain. Our observation that epithelial β-CYA-depleted cells become polynucleated, is compatible with the assumption that β-CYA is involved in contractile-ring formation.

The contractile phenotype observed in γ-CYA-depleted cells is characterized by a reduction of protrusive γ-CYA-rich structures and also by an enrichment of α-SMA in stress fibers. This increase in α-SMA expression could be a consequence of the modulation of fibroblasts towards the myofibroblast phenotype (Hinz et al., 2002). However, we cannot exclude that the observed α-SMA upregulation is the result of a compensation of γ-CYA downregulation.

In conclusion, our results reinforce and extend the possibility that actin isoforms are involved in distinct cellular functions. Such an assumption, based on the evolutionary conservation of sequence differences among different isoforms, has received support from studies of muscle isoforms (Chaponnier and Gabbiani, 2004; Lambrechts et al., 2004). Previous work has shown that α-SMA plays a crucial role in tension production by myofibroblast stress fibers (Hinz et al., 2002). Taken together, our results reveal a crucial new aspect of CYA organization and support a preferential role in contractile activities for β-CYA and in the formation of the compliant filamentous networks necessary for cell-shape flexibility and motile activity for γ-CYA.

Materials and Methods

Production and characterization of antibodies

Anti-β- and γ-CYA mAbs were prepared following the Repetitive Immunizations at Multiple Sites strategy (RIMMS) (Kilpatrick et al., 1997). Mice were immunized with the N-terminal nonapeptide of β-CYA (Ac-DDDIAALVV) or γ-CYA (Ac-EEEIAALVI) conjugated with keyhole limpet hemocyanin. Hybridoma cells were screened by triple ELISA, using 96-well plates coated with α-SMA, β-CYA and γ-CYA BSA-conjugated peptides. Selected hybridomas were cloned twice by limited dilution and characterized by immunofluorescence staining using rat lip cryostat sections; by western blotting using platelets, heart, aorta, skeletal muscle, gizzard extracts, HSCF and MDCK total-cell extracts after 1D SDS-PAGE and using HSCF, MDCK, rat aorta and purified chicken gizzard actin after 2D-PAGE; and by blocking

assays using the N-terminal peptides of the γ-CYA isoforms (Chaponnier et al., 1995; Clement et al., 1999) on rat lip cryostat sections (immunofluorescence) and on aorta extracts (western blotting). The six isoform peptides, coupled to MBS-activated BSA (Chaponnier et al., 1995), were subjected to SDS-PAGE and western blotting.

Electrophoretic and immunoblot analysis

Proteins were extracted in Sample Buffer (Laemmli, 1970) for 1D SDS-PAGE or in Iso buffer for 2D-PAGE (Skalli et al., 1987). Cell lysates were run on 10% SDS-PAGE or for 2D-PAGE using 2% Pharmalyte, pH 4-6.5 (GE Healthcare, Munich, Germany), for the first dimension and electroblotted to nitrocellulose membrane. Membranes were incubated with the following mAbs: anti-β-CYA (4C2), anti-γ-CYA (2A3), anti-α-SMA [anti-αsm-1, clone 1A4, (Skalli et al., 1986)], anti-total-actin (pan-actin, clone C4; Chemicon, Temecula, CA), and anti-vimentin (clone V9; Dako, Copenhagen, Denmark) or anti-α-tubulin (clone B-5-1-2; Sigma, Buchs, Switzerland), followed by the incubation with HRP-conjugated goat anti-mouse IgG (Jackson ImmunoResearch Laboratories, West Grove, PA). HRP activity was developed using the ECL system (GE Healthcare), and blots were scanned and quantified using densitometric analysis (Optiquant software; Packard Instrument, Meriden, CT).

Cell culture and treatment

HSCFs, rat lung fibroblasts, rat subcutaneous fibroblasts and pig aortic endothelial cells were obtained as previously described (Desmouliere et al., 1993). The following cell lines were used: human HaCaT, rat kangaroo kidney PtK2 and MDCK, human embryonic fibroblasts (WI38 and their transformed counterparts WI38-VA13), human embryonic lung fibroblasts (HEL) and rat embryonic fibroblasts (REF-52). Cells were cultured in DMEM-Glutamax (Gibco, Invitrogen, Basel, Switzerland) and 10% FCS (Seromed, Biochrom KG, Berlin, Germany) at 37°C with 5% CO_2. Cells on glass coverslips were cultured for 3-6 hours to 3 days. For wound assays, confluent cell monolayers were scratched with a 200-μl pipette tip. In inhibition assays, spreading cells were treated with selective inhibitors of Rho-kinase (Y-27632, 10 μM for 2 hours; Calbiochem, San Diego, CA), of Rac1 GDP-GTP exchange activity (NSC23766, 50-100 μM for 4 hours; Calbiochem), of non-muscle myosin II (blebbistatin, 25 μM for 4 hours; Biomol International, Plymouth Meeting, PA), of N-WASP (wiskostatin, 5-10 μM for 30 minutes; Calbiochem) and with actin-polymerization-interfering agents (CD, 0.1 μM for 30 minutes and LatA, 0.1-0.2 μM for 30 minutes; both from Calbiochem). All inhibitors were added during the final period of the 7-hour spreading time.

Immunofluorescence and confocal laser scanning microscopy

Cells were rinsed with DMEM containing 20 mM HEPES at 37°C, fixed in 1% PFA in prewarmed DMEM for 30 minutes and treated for 5 minutes with MeOH at –20°C. Cells were incubated with the following primary mAbs: newly developed anti-β-CYA (mAb 4C2, IgG1) and anti-γ-CYA (mAb 2A3, IgG2b); commercially available anti-β-CYA mAbs AC-74 (IgG2a) [Sigma (Gimona et al., 1994)]; anti-αsm-1 (Skalli et al., 1986); anti-VASP (clone IE273, ImmunoGlobe, Germany); anti-tropomyosin, (clone TM311, Sigma); and rabbit polyclonal Abs: anti-p34-Arc (Upstate, Millipore, Zug, Switzerland), anti-α-spectrin (Biomakor, Rehovot, Israel) and anti-non-muscle myosin II heavy chain A (MHC-A, Covance Research Products, Emeryville, CA). The following secondary Abs were used: FITC- and TRITC-conjugated goat anti-mouse IgG1, TRITC-conjugated goat anti-mouse IgG2b (Southern Biotechnology, Associates, Birmingham, AL), Alexa-Fluor-488-conjugated goat anti-mouse IgG (Molecular Probes, Invitrogen) and TRITC-conjugated goat anti-rabbit (Jackson). DRAQ5 (Biostatus, Leicestershire, UK) was used for nuclear staining.

Images were acquired using a confocal microscope (LSM510, Zeiss, Oberkochen, Germany) equipped with oil-immersion objectives (Plan-Neofluar 63× 1.4 and Plan-Fluar 100× 1.45, Zeiss). Single optical sections were scanned with ~1-μm thickness near the basal level of the cell. For serial optical sections stacks with *z*-step of 0.3-0.5 μm were collected. Images were processed using Adobe Photoshop software.

REF-52 cells were transfected with the β-actin–EGFP construct as previously reported (Clement et al., 2005).

siRNA transfection

siRNAs targeting the sequence of human β-actin (NM_001101) [β-actin siRNA1: 5′-AATGAAGATCAAGATCATTGC-3′, (Harborth et al., 2001); β-actin siRNA2: 5′-TAGCATTGCTTTCGTGTAAAT-3′ and β-actin siRNA3: 5′-CAAATATGAG-ATGCATTGTTA-3′] and γ-actin (NM_001614) [γ-actin siRNA1: 5′-AAGA-GATCGCCGCGCTGGTCA-3′ (Harborth et al., 2001) and γ-actin siRNA2: 5′-CAGCAACACGTCATTGTGTAA-3′] were purchased from Qiagen (Hombrechtikon, Switzerland).

Cells were transfected with 50-100 nM siRNA using Lipofectamine 2000 (Invitrogen). Transfection efficiency (80-90%) was estimated using BLOCK-iT (Invitrogen).

Cell morphometry

HSCFs were transfected with siRNA, replated at single-cell density onto glass coverslips 48 hours after transfection, and stained for β-CYA and γ-CYA 72 hours after transfection.

ImageJ software (NIH, http://rsb.info.nih.gov/ij/) was used to trace cell outlines and measure cell surface area (*A*) and perimeter (*P*). Circularity was calculated as a normalized ratio of *A* to *P* (circularity=$4\pi A/P^2$), with a value of 1 representing a perfect circle and a value close to 0 representing more elliptical or elongated surfaces.

Live-cell imaging

Live-cell imaging was performed on an Axiovert 100M microscope (Zeiss) at 37°C with 5% CO_2, using a CCD camera (Hamamatsu Photonics, Massy, France) operated by Openlab software (Improvision, Basel, Switzerland). HSCFs were transfected with 50 nM siRNA and 50 nM BLOCK-iT Fluorescent Oligo (Invitrogen) to label transfected cells and plated at single-cell density onto glass-bottom dishes (MatTek, Ashland, MA). Images for kymography analysis were taken with a 40× 0.75 Plan-Neofluar objective every 2 seconds for 5 minutes. Kymographs were produced from image sequences as described (Hinz et al., 1999) using MetaMorph software (Universal Imaging, West Chester, PA).

Long-timescale migration assays were performed using ImageXpress^{Micro} system (Molecular Devices, Ismaning, Germany) at 37°C with 5% CO_2. HSCFs were transfected with 50 nM siRNA and 50 nM BLOCK-iT for transfection control before and after tracking, plated 48 hours after transfection at single-cell density in black-walled, clear-bottomed 96-well plates (Costar 3904; Acton, MA). For motility studies, images from cells in eight separate wells for each condition were taken at 72 hours post-transfection with a 10× 0.50 objective (W.D 1.20 mm S Fluor, Nikon, Küsnacht, Switzerland) every 5 minutes for 13 hours. Average speed (μm/hour, calculated as total track distance divided by total time of experiment), speed (μm/hour, calculated during periods of cell movement, periods with speed equal to 0 were not taken), absolute angle, total track distance and direct distance were determined by tracking the positions of cell nuclei using the Track Point function of MetaMorph. *D*:*T* ratio represents the ratio of the direct distance from start to end point (*D*) divided by the total track distance (*T*). Data are presented from three independent experiments (35-40 cells for each experiment).

Statistical analysis

Results are expressed as mean ± s.e.m. of at least three independent experiments. For statistical comparisons, results were analyzed by Student's *t*-test. Values of $P<0.001$ (***), $P<0.01$ (**) and $P<0.05$ (*) were considered statistically significant.

This work was supported by research grants from the Swiss National Science Foundation (3100A0-109879 to C.C. and PMPDA-102408 to S.C.), an EMBO fellowship to I.Z., and Russian Foundation of Basic Investigation (grant 06-04-49214a) and financial support from the Faculty of Medicine, University of Geneva to V.D. We gratefully acknowledge Giuseppe Celetta and Anita Hiltbrunner for their invaluable involvement in producing the mAbs and technical help; Pierre-Alain Rüttimann for scheme drawing; Lionel Fontao (Department of Dermatology, University Hospital of Geneva, Switzerland) for providing HaCaT cells; and Serge Arnaudeau, Olivier Brun and Sergei Startchik (Bioimaging Core Facility, Faculty of Medicine, Geneva, Switzerland) for their help and advices in using microscope settings and in analyzing the morphometric and motility data.

References

Abercrombie, M., Heaysman, J. E. and Pegrum, S. M. (1970). The locomotion of fibroblasts in culture. I. Movements of the leading edge. *Exp. Cell Res.* **59**, 393-398.

Abercrombie, M., Heaysman, J. E. and Pegrum, S. M. (1971). The locomotion of fibroblasts in culture. IV. Electron microscopy of the leading lamella. *Exp. Cell Res.* **67**, 359-367.

Antecol, M. H., Darveau, A., Sonenberg, N. and Mukherjee, B. B. (1986). Altered biochemical properties of actin in normal skin fibroblasts from individuals predisposed to dominantly inherited cancers. *Cancer Res.* **46**, 1867-1873.

Bassell, G. J., Zhang, H., Byrd, A. L., Femino, A. M., Singer, R. H., Taneja, K. L., Lifshitz, L. M., Herman, I. M. and Kosik, K. S. (1998). Sorting of beta-actin mRNA and protein to neurites and growth cones in culture. *J. Neurosci.* **18**, 251-265.

Chaponnier, C. and Gabbiani, G. (2004). Pathological situations characterized by altered actin isoform expression. *J. Pathol.* **204**, 386-395.

Chaponnier, C., Goethals, M., Janmey, P. A., Gabbiani, F., Gabbiani, G. and Vandekerckhove, J. (1995). The specific NH2-terminal sequence Ac-EEED of alpha-smooth muscle actin plays a role in polymerization in vitro and in vivo. *J. Cell Biol.* **130**, 887-895.

Chhabra, E. S. and Higgs, H. N. (2007). The many faces of actin: matching assembly factors with cellular structures. *Nat. Cell Biol.* **9**, 1110-1121.

Clement, S., Chaponnier, C. and Gabbiani, G. (1999). A subpopulation of cardiomyocytes expressing alpha-skeletal actin is identified by a specific polyclonal antibody. *Circ. Res.* **85**, e51-e58.

Clement, S., Hinz, B., Dugina, V., Gabbiani, G. and Chaponnier, C. (2005). The N-terminal Ac-EEED sequence plays a role in alpha-smooth-muscle actin incorporation into stress fibers. *J. Cell Sci.* **118**, 1395-1404.

Condeelis, J. and Singer, R. H. (2005). How and why does beta-actin mRNA target? *Biol. Cell* **97**, 97-110.

Desmouliere, A., Geinoz, A., Gabbiani, F. and Gabbiani, G. (1993). Transforming growth factor-beta 1 induces alpha-smooth muscle actin expression in granulation tissue myofibroblasts and in quiescent and growing cultured fibroblasts. *J. Cell Biol.* **122**, 103-111.

Even-Ram, S., Doyle, A. D., Conti, M. A., Matsumoto, K., Adelstein, R. S. and Yamada, K. M. (2007). Myosin IIA regulates cell motility and actomyosin-microtubule crosstalk. *Nat. Cell Biol.* **9**, 299-309.

Fenteany, G., Janmey, P. A. and Stossel, T. P. (2000). Signaling pathways and cell mechanics involved in wound closure by epithelial cell sheets. *Curr. Biol.* **10**, 831-838.

Gao, Y., Dickerson, J. B., Guo, F., Zheng, J. and Zheng, Y. (2004). Rational design and characterization of a Rac GTPase-specific small molecule inhibitor. *Proc. Natl. Acad. Sci. USA* **101**, 7618-7623.

Gimona, M., Vandekerckhove, J., Goethals, M., Herzog, M., Lando, Z. and Small, J. V. (1994). Beta-actin specific monoclonal antibody. *Cell Motil. Cytoskeleton* **27**, 108-116.

Goeckeler, Z. M., Bridgman, P. C. and Wysolmerski, R. B. (2008). Nonmuscle myosin II is responsible for maintaining endothelial cell basal tone and stress fiber integrity. *Am. J. Physiol. Cell Physiol.* **295**, C994-C1006.

Hanft, L. M., Rybakova, I. N., Patel, J. R., Rafael-Fortney, J. A. and Ervasti, J. M. (2006). Cytoplasmic gamma-actin contributes to a compensatory remodeling response in dystrophin-deficient muscle. *Proc. Natl. Acad. Sci. USA* **103**, 5385-5390.

Harborth, J., Elbashir, S. M., Bechert, K., Tuschl, T. and Weber, K. (2001). Identification of essential genes in cultured mammalian cells using small interfering RNAs. *J. Cell Sci.* **114**, 4557-4565.

Heath, J. P. and Holifield, B. F. (1993). On the mechanisms of cortical actin flow and its role in cytoskeletal organisation of fibroblasts. *Symp. Soc. Exp. Biol.* **47**, 35-56.

Hill, M. A. and Gunning, P. (1993). Beta and gamma actin mRNAs are differentially located within myoblasts. *J. Cell Biol.* **122**, 825-832.

Hinz, B., Alt, W., Johnen, C., Herzog, V. and Kaiser, H. W. (1999). Quantifying lamella dynamics of cultured cells by SACED, a new computer-assisted motion analysis. *Exp. Cell Res.* **251**, 234-243.

Hinz, B., Gabbiani, G. and Chaponnier, C. (2002). The NH2-terminal peptide of alpha-smooth muscle actin inhibits force generation by the myofibroblast in vitro and in vivo. *J. Cell Biol.* **157**, 657-663.

Hofer, D., Ness, W. and Drenckhahn, D. (1997). Sorting of actin isoforms in chicken auditory hair cells. *J. Cell Sci.* **110**, 765-770.

Hoock, T. C., Newcomb, P. M. and Herman, I. M. (1991). Beta actin and its mRNA are localized at the plasma membrane and the regions of moving cytoplasm during the cellular response to injury. *J. Cell Biol.* **112**, 653-664.

Kilpatrick, K. E., Wring, S. A., Walker, D. H., Macklin, M. D., Payne, J. A., Su, J. L., Champion, B. R., Caterson, B. and McIntyre, G. D. (1997). Rapid development of affinity matured monoclonal antibodies using RIMMS. *Hybridoma* **16**, 381-389.

Kislauskis, E. H., Zhu, X. and Singer, R. H. (1994). Sequences responsible for intracellular localization of beta-actin messenger RNA also affect cell phenotype. *J. Cell Biol.* **127**, 441-451.

Kovacs, M., Toth, J., Hetenyi, C., Malnasi-Csizmadia, A. and Sellers, J. R. (2004). Mechanism of blebbistatin inhibition of myosin II. *J. Biol. Chem.* **279**, 35557-35563.

Laemmli, U. K. (1970). Cleavage of structural proteins during the assembly of the head of bacteriophage T4. *Nature* **227**, 680-685.

Lambrechts, A., Van Troys, M. and Ampe, C. (2004). The actin cytoskeleton in normal and pathological cell motility. *Int. J. Biochem. Cell Biol.* **36**, 1890-1909.

Latham, V. M., Yu, E. H., Tullio, A. N., Adelstein, R. S. and Singer, R. H. (2001). A Rho-dependent signaling pathway operating through myosin localizes beta-actin mRNA in fibroblasts. *Curr. Biol.* **11**, 1010-1016.

Lauffenburger, D. A. and Horwitz, A. F. (1996). Cell migration: a physically integrated molecular process. *Cell* **84**, 359-369.

Lunn, J. A., Wong, H., Rozengurt, E. and Walsh, J. H. (2000). Requirement of cortical actin organization for bombesin, endothelin, and EGF receptor internalization. *Am. J. Physiol. Cell Physiol.* **279**, C2019-C2027.

Nelson, W. J. (2003). Adaptation of core mechanisms to generate cell polarity. *Nature* **422**, 766-774.

Otey, C. A., Kalnoski, M. H., Lessard, J. L. and Bulinski, J. C. (1986). Immunolocalization of the gamma isoform of nonmuscle actin in cultured cells. *J. Cell Biol.* **102**, 1726-1737.

Pawlak, G. and Helfman, D. M. (2001). Cytoskeletal changes in cell transformation and tumorigenesis. *Curr. Opin. Genet. Dev.* **11**, 41-47.

Pellegrin, S. and Mellor, H. (2007). Actin stress fibres. *J. Cell Sci.* **120**, 3491-3499.

Peterson, J. R., Bickford, L. C., Morgan, D., Kim, A. S., Ouerfelli, O., Kirschner, M. W. and Rosen, M. K. (2004). Chemical inhibition of N-WASP by stabilization of a native autoinhibited conformation. *Nat. Struct. Mol. Biol.* **11**, 747-755.

Pollack, R., Osborn, M. and Weber, K. (1975). Patterns of organization of actin and myosin in normal and transformed cultured cells. *Proc. Natl. Acad. Sci. USA* **72**, 994-998.

Revenu, C., Athman, R., Robine, S. and Louvard, D. (2004). The co-workers of actin filaments: from cell structures to signals. *Nat. Rev. Mol. Cell Biol.* **5**, 635-646.

Ridley, A. J. and Hall, A. (1992). The small GTP-binding protein rho regulates the assembly of focal adhesions and actin stress fibers in response to growth factors. *Cell* **70**, 389-399.

Ridley, A. J., Paterson, H. F., Johnston, C. L., Diekmann, D. and Hall, A. (1992). The small GTP-binding protein rac regulates growth factor-induced membrane ruffling. *Cell* **70**, 401-410.

Ridley, A. J., Schwartz, M. A., Burridge, K., Firtel, R. A., Ginsberg, M. H., Borisy, G., Parsons, J. T. and Horwitz, A. R. (2003). Cell migration: integrating signals from front to back. *Science* **302**, 1704-1709.

Rubin, R. W., Warren, R. H., Lukeman, D. S. and Clements, E. (1978). Actin content and organization in normal and transformed cells in culture. *J. Cell Biol.* **78**, 28-35.

Sandquist, J. C., Swenson, K. I., Demali, K. A., Burridge, K. and Means, A. R. (2006). Rho kinase differentially regulates phosphorylation of nonmuscle myosin II isoforms A and B during cell rounding and migration. *J. Biol. Chem.* **281**, 35873-35883.

Sarmiento, C., Wang, W., Dovas, A., Yamaguchi, H., Sidani, M., El-Sibai, M., Desmarais, V., Holman, H. A., Kitchen, S., Backer, J. M. et al. (2008). WASP family members and formin proteins coordinate regulation of cell protrusions in carcinoma cells. *J. Cell Biol.* **180**, 1245-1260.

Schevzov, G., Vrhovski, B., Bryce, N. S., Elmir, S., Qiu, M. R., O'Neill, G. M., Yang, N., Verrills, N. M., Kavallaris, M. and Gunning, P. W. (2005). Tissue-specific tropomyosin isoform composition. *J. Histochem. Cytochem.* **53**, 557-570.

Shawlot, W., Deng, J. M., Fohn, L. E. and Behringer, R. R. (1998). Restricted beta-galactosidase expression of a hygromycin-lacZ gene targeted to the beta-actin locus and embryonic lethality of beta-actin mutant mice. *Transgenic Res.* **7**, 95-103.

Skalli, O., Ropraz, P., Trzeciak, A., Benzonana, G., Gillessen, D. and Gabbiani, G. (1986). A monoclonal antibody against alpha-smooth muscle actin: a new probe for smooth muscle differentiation. *J. Cell Biol.* **103**, 2787-2796.

Skalli, O., Vandekerckhove, J. and Gabbiani, G. (1987). Actin-isoform pattern as a marker of normal or pathological smooth-muscle and fibroblastic tissues. *Differentiation* **33**, 232-238.

Small, J. V. (1981). Organization of actin in the leading edge of cultured cells: influence of osmium tetroxide and dehydration on the ultrastructure of actin meshworks. *J. Cell Biol.* **91**, 695-705.

Small, J. V., Rottner, K., Kaverina, I. and Anderson, K. I. (1998). Assembling an actin cytoskeleton for cell attachment and movement. *Biochim. Biophys. Acta* **1404**, 271-281.

Sonnemann, K. J., Fitzsimons, D. P., Patel, J. R., Liu, Y., Schneider, M. F., Moss, R. L. and Ervasti, J. M. (2006). Cytoplasmic gamma-actin is not required for skeletal muscle development but its absence leads to a progressive myopathy. *Dev. Cell* **11**, 387-397.

Spector, I., Shochet, N. R., Blasberger, D. and Kashman, Y. (1989). Latrunculins-novel marine macrolides that disrupt microfilament organization and affect cell growth: I. Comparison with cytochalasin D. *Cell Motil. Cytoskeleton* **13**, 127-144.

Straight, A. F., Cheung, A., Limouze, J., Chen, I., Westwood, N. J., Sellers, J. R. and Mitchison, T. J. (2003). Dissecting temporal and spatial control of cytokinesis with a myosin II Inhibitor. *Science* **299**, 1743-1747.

Svitkina, T. M. and Borisy, G. G. (1999). Arp2/3 complex and actin depolymerizing factor/cofilin in dendritic organization and treadmilling of actin filament array in lamellipodia. *J. Cell Biol.* **145**, 1009-1026.

Svitkina, T. M., Verkhovsky, A. B. and Borisy, G. G. (1995). Improved procedures for electron microscopic visualization of the cytoskeleton of cultured cells. *J. Struct. Biol.* **115**, 290-303.

Uehata, M., Ishizaki, T., Satoh, H., Ono, T., Kawahara, T., Morishita, T., Tamakawa, H., Yamagami, K., Inui, J., Maekawa, M. et al. (1997). Calcium sensitization of smooth muscle mediated by a Rho-associated protein kinase in hypertension. *Nature* **389**, 990-994.

Vandekerckhove, J. and Weber, K. (1978). At least six different actins are expressed in a higher mammal: an analysis based on the amino acid sequence of the amino-terminal tryptic peptide. *J. Mol. Biol.* **126**, 783-802.

Verderame, M., Alcorta, D., Egnor, M., Smith, K. and Pollack, R. (1980). Cytoskeletal F-actin patterns quantitated with fluorescein isothiocyanate-phalloidin in normal and transformed cells. *Proc. Natl. Acad. Sci. USA* **77**, 6624-6628.

Watanabe, H., Kislauskis, E. H., Mackay, C. A., Mason-Savas, A. and Marks, S. C., Jr (1998). Actin mRNA isoforms are differentially sorted in normal osteoblasts and sorting is altered in osteoblasts from a skeletal mutation in the rat. *J. Cell Sci.* **111**, 1287-1292.

Winder, S. J. and Ayscough, K. R. (2005). Actin-binding proteins. *J. Cell Sci.* **118**, 651-654.

Yao, X., Chaponnier, C., Gabbiani, G. and Forte, J. G. (1995). Polarized distribution of actin isoforms in gastric parietal cells. *Mol. Biol. Cell* **6**, 541-557.

Yeaman, C., Grindstaff, K. K. and Nelson, W. J. (1999). New perspectives on mechanisms involved in generating epithelial cell polarity. *Physiol. Rev.* **79**, 73-98.